Acta Crystallographica Section D
Biological Crystallography
ISSN 0907-4449

W3Y single mutant of rubredoxin from *Pyrococcus furiosus*: a preliminary time-of-flight neutron study

Xinmin Li,[a] Paul Langan,[a]* Robert Bau,[b] Irina Tsyba,[b] Francis E. Jenney Jr,[c] Michael W. W. Adams[c] and Benno P. Schoenborn[a]

[a]Bioscience Division, Los Alamos National Laboratory, Los Alamos, NM 87545, USA, [b]Chemistry Department, University of Southern Cailfornia, Los Angeles, CA 90089, USA, and [c]Department of Biochemistry, University of Georgia, Athens, GA 30602, USA

Correspondence e-mail: langan_paul@lanl.gov

Received 13 August 2003
Accepted 21 October 2003

Rubredoxin from the hyperthermophilic archaeon *Pyrococcus furiosus* maintains its native structure at high temperatures (373 K). In order to investigate the role of hydrogen bonding, hydration and chain dynamics in this thermostability, wavelength-resolved Laue neutron diffraction data have been collected from the W3Y single mutant (Trp3→Tyr3) on the spallation neutron protein crystallography station (PCS) at Los Alamos Neutron Science Center. Data were measured at room temperature from nine crystal settings, each of approximately 12 h duration. The total data-measurement period was less than 5 d from a single crystal that had undergone H_2O/D_2O exchange. The nominal resolution of the data is 2.1 Å.

1. Introduction

Pyrococcus furiosus is a hyperthermophilic archaeon found in shallow marine geothermal vents (Fiala & Stetter, 1986). Rubredoxin from *P. furiosus* (PfRd) maintains its native structure at high temperatures (373 K) for several hours, unlike rubredoxin from many other organisms, for example the mesophile *Clostridium pasteurianum* (CpRd), which denatures more quickly (Zartler *et al.*, 2001). Although rubredoxin has been proposed to play an electron-transfer role in many different pathways (Jenney & Adams, 2001), there has as yet been no definitive *in vivo* proof of its function. Rubredoxin has 53 amino-acid residues arranged in three β-sheets folded around a core of hydrophobic side groups (Bau *et al.*, 1998). Four cysteine residues from two opposing β-sheets coordinate an Fe-atom cofactor. It has been suggested that the thermostability of PfRd may be related to its eight-residue hydrophobic core. Three of these residues are different in CpRd. The difference at residue 3 (Trp3 in PfRd and Tyr3 in CpRd) is particularly interesting, because not only is the side group part of the hydrophobic core, but the residue is also part of a β-sheet that appears to serve a number of structural roles. These structural roles include clamping the Fe atom and tying down the C-terminal and N-terminal strands. PfRd in which the three residues of the hydrophobic core have been mutated to those of CpRd is significantly less stable than wild-type PfRd at low pH. However, NMR analysis of wild-type PfRd and the triple mutant (Zartler *et al.*, 2001) and ultrahigh-resolution 100 K X-ray structures of the wild-type PfRd (0.95 Å) and CpRd (1.1 Å) have revealed no striking differences (Bau *et al.*, 1998; Dauter *et al.*, 1996).

The present study is the latest in a series designed to determine the contribution of hydrogen bonding, hydration and dynamics to the thermostability of PfRd (Kurihara *et al.*, 2001; Chatake *et al.*, 2002). It has been difficult to directly determine the positions of H atoms in the X-ray structures of rubredoxin and none have been reported for the labile positions in the ultrahigh-resolution structure of PfRd (Bau *et al.*, 1998). Neutron diffraction has been shown to be a powerful technique for locating H atoms even at medium resolution. What is more, neutron diffraction data can be collected at room temperature, rather than the cryo-temperatures required for high-resolution X-ray protein crystallography, because thermal neutrons cause little direct radiation damage. Hydrogen has a relatively strong but negative neutron scattering length; thus, H atoms are located as negative density peaks in neutron Fourier maps. Deuterium (D), an isotope of H, also has a relatively strong neutron scattering length but, like those of O, C, N, Fe and S atoms, it is positive. D atoms are therefore located as positive density peaks in neutron maps.

By soaking rubredoxin crystals in mother liquor containing D_2O rather than H_2O, accessible labile H atoms can be replaced by D atoms. This increases the scattering power of the crystal for neutrons at medium resolution, where the negative scattering density of H atoms tends to cancel out the positive density of other atoms. The positions of individual D atoms and the orientation of D_2O molecules can be determined even at a resolution of 2.2 Å after H_2O/D_2O exchange. This exchange also

© 2004 International Union of Crystallography
Printed in Denmark – all rights reserved

Table 1
Data-collection parameters for rubredoxin single mutant W3Y.

Space group	$P2_12_12_1$
Unit-cell parameters† (Å)	a = 34.32, b = 35.31, c = 44.23
Wavelength range (Å)	0.6–7
Station	PCS
Temperature (K)	295
Crystal settings	9
Average time per setting (h)	12
Observed reflections	10315
Observed reflections, d > 2.1 Å	5357
Unique reflections, d > 2.1 Å	2184

† From X-ray diffraction.

Table 2
I/σ, I/S_d, R_{merge} ($I > 1.5\sigma$) and completeness (%Comp) *versus* resolution for the rubredoxin single mutant.

The cumulative R_{merge} and completeness are also given (CumR_{merge}, Cum%Comp). S_d corresponds to the standard deviation in merging reflections as opposed to σ, the error involved in measuring individual intensities.

Resolution	No. of reflections	%Comp	Cum%Comp	R_{merge}	CumR_{merge}	$\langle I/\sigma \rangle$	$\langle I/S_d \rangle$
∞–6.64	208	85.2	85.2	0.076	0.076	7.9	21.5
6.64–4.70	426	80.3	82.0	0.093	0.086	6.6	17.5
4.70–3.83	522	79.4	80.8	0.104	0.094	5.5	14.8
3.83–3.32	558	74.5	78.6	0.123	0.102	3.7	11.9
3.32–2.97	587	70.2	76.2	0.156	0.111	2.0	8.6
2.97–2.71	606	69.6	74.6	0.131	0.113	5.1	5.4
2.71–2.51	626	66.8	73.0	0.213	0.118	2.5	3.4
2.51–2.35	607	64.3	71.4	0.192	0.120	2.8	2.8
2.35–2.21	608	65.9	70.6	0.231	0.123	2.8	2.6
2.21–2.10	609	62.8	69.4	0.236	0.125	2.1	2.0

reduces incoherent scattering from hydrogen in the crystal, which tends to contribute to background scattering and reduces the diffraction signal. Finally, and of particular significance in this study, H_2O/D_2O exchange can be used to probe dynamics. The extent of H/D exchange in main-chain amide groups, as determined in neutron Fourier maps, directly reflects local dynamics along the rubredoxin backbone chain (Hiller *et al.*, 1997; Hernandez *et al.*, 2000; Zartler *et al.*, 2001).

The neutron structures of the wild-type PfRd and a triple mutant have already been determined using data collected on BIX-3 at JAERI (Kurihara *et al.*, 2001; Chatake *et al.*, 2002). This preliminary report concerns the neutron structure of the W3Y (Trp3→Tyr3) single-mutant PfRd determined from data collected at the spallation neutron Protein Crystallography Station (PCS) at Los Alamos Neutron Science Center.

2. Materials and methods

2.1. Crystallization and deuteration

Crystallization was carried out at the University of Southern California from a D_2O solution containing 40 mg ml^{-1} protein (∼6 m*M* PfRd) dissolved in 50 m*M* Tris/Tris–DCl buffer (pH 8.0, pD 8.4) and 0.3 *M* NaCl. The sitting-drop method was used with 40 µl drops, 3.6 *M* sodium/potassium phosphate (pH 6.6, pD 7.0) in D_2O as precipitant and with a sample-to-precipitant ratio of 3:1 or 4:1. Crystals were harvested, crushed and used as seeds. The stock seed solution was diluted to the point where only one or two crystals appeared in the subsequent drop. When more that one crystal appeared after seeding, all but one were redissolved by adding a small amount of D_2O. Crystals grew for about two months and reached sizes as large as 4 mm^3 at room temperature. Crystals were stabilized during growth by increasing the phosphate concentration. The crystals were transported to the Bioscience division at Los Alamos in 3.8–4 *M* phosphate solutions; they were then mounted and sealed, along with some mother liquor, in clear fused-quartz capillaries supplied by Vitrocom with an inner diameter of 2.0 mm. A number of crystals were tested for neutron diffraction quality with relatively short exposures of 1 h duration. A crystal with longest dimension 1.5 mm was used for data collection.

2.2. Data measurement

Diffraction data were collected on the spallation neutron protein crystallography station (PCS) at Los Alamos Neutron Science Center (Langan *et al.*, 2004). At the spallation source, neutrons are produced in pulses at a rate of 20 Hz. The neutrons are time-stamped and travel as a function of their energy down the beamline. By recording the TOF information from the initial pulse at the source to detection, the wavelength of a neutron can be calculated. The Laue data collected on the PCS are therefore resolved in wavelength. The capillary containing the crystal and its deuterated mother liquor was mounted on the PCS κ-circle goniometer and wavelength-resolved Laue patterns were collected at nine different crystal orientations at room temperature, as summarized in Table 1.

The strategy used was to collect data from an octant of reciprocal space by scanning the crystal around its spindle axis in three steps of 30° in φ. The cylindrical detector was positioned in the straight-through orientation so that it subtended ±60° in its horizontal curved 2θ plane and ±8° in its vertical flat direction. The detector was not moved between crystal settings and the sample-to-detector distance of 70 cm corresponded to the cylindrical radius of the detector. The exposure time was 12 h at each crystal setting. Because of the limited coverage of the detector in the vertical direction, the crystal should have been reoriented four times using the κ and ω circles of the goniometer, with φ scans being collected at each orientation. However, because of lack of time only three reorientations were carried out.

The data over the wavelength range 0.6–7 Å were processed using a version of *d*TREK* (Pflugrath, 1999) modified for wavelength-resolved neutron Laue protein crystallography (Langan & Greene, 2004). The processed intensities from all crystal settings were scaled and wavelength-normalized using *LAUENORM* (Campbell *et al.*, 1986; Helliwell *et al.*, 1989). In order to obtain reasonable values for R_{merge}, the wavelength range was narrowed to 0.8–4.5 Å and only reflections with $I > 3\sigma$ were used in determining the wavelength-scaling normalization curve. Reflections in this wavelength range were binned into ten wavelength intervals and the normalization curve was determined from a Chebyshev

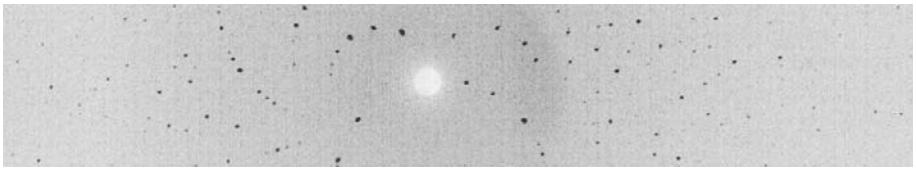

Figure 1
Wavelength-resolved Laue diffraction data collected from PfRd single mutant displayed using *d*TREK* (Pflugrath, 1999; Langan & Greene, 2004). Although the data are three-dimensional [two detector spatial dimensions and a third wavelength (TOF) dimension], a two-dimensional image has been constructed by displaying at each detector pixel position the maximum value of that pixel over all wavelengths.

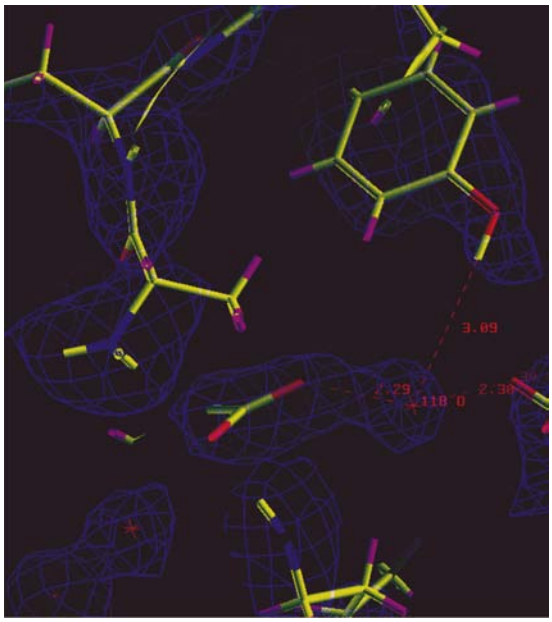

Figure 2
A section of the 2.1 Å $2F_o - F_c\,\sigma_A$ map in the region of the Tyr3 mutation site, calculated without including the labile H/D-atom positions in the phases. Positive density associated with the Tyr3 hydroxyl group (indicated by the white arrow) clearly indicates the orientation of this group and that the labile H atom has been replaced by a D atom.

polynomial of order 5. The data were output in unmerged form so that *SCALA* (Evans, 1997) could be used for statistical analysis.

3. Results and discussion

A representation of the data collected at one crystal setting is shown in Fig. 1. In this figure, the data collected at different wavelengths has been projected in order to construct an image similar to a conventional Laue diffraction pattern. The values of $R_{\rm merge}$ calculated using the program *LAUENORM* for the data measured at all crystal settings are 0.131 for all measurements of a reflection (2920 reflections), 0.110 for measurements of a reflection of the same sign (2029 reflections) and 0.096 for all measurements of a reflection of the same sign and within λ = 0.1 Å (277 reflections). Table 2 shows the values of $R_{\rm merge}$ and completeness as a function of resolution calculated using the program *SCALA*. The value of I/σ flattened off beyond 2.1 Å, suggesting that this is about the limit of diffraction. The completeness of the data in the outer resolution shell (2.1–2.2 Å) is 63%. In the lower resolution shells the values of $I/S_{\rm d}$ are larger than the values of I/σ, where $S_{\rm d}$ corresponds to the standard deviation in merging reflections as opposed to σ, the error involved in measuring individual intensities. This is probably owing to the high redundancy of data (2.5), which is a feature of Laue diffraction, and perhaps also to an overestimation of σ for weak reflections.

The data-collection time of 4–5 d using the PCS is relatively short compared with the weeks or even months typically required for neutron protein crystallography. This is largely owing to the use of spallation neutrons and the wavelength-resolved Laue technique, which has all of the advantages of the conventional Laue method, including rapid coverage of reciprocal space, but does not suffer to the same extent from reflection overlap and background accumulation because the reflections and the background scattering are resolved in wavelength. The quality of the data and the power of neutron diffraction for locating H atoms at medium resolution are illustrated in Fig. 2, which shows a section of a 2.1 Å $2F_o - F_c\,\sigma_A$ map in the region of Tyr3 calculated without including the labile H/D-atom positions in the phases. Density associated with the hydroxyl group clearly indicates the orientation of this group and that the labile H atom has been replaced by a D atom. Full analysis of this data reveals a wealth of information on hydration and backbone-chain dynamics and will be reported elsewhere.

The PCS is funded by the Office of Science and the Office of Biological and Environmental Research of the US Department of Energy. RB, MA and FJ thank the National Science Foundation for partial support of this research.

References

Bau, R., Rees, D. C., Kurtz, D. M., Scott, R. A., Huang, H. S., Adams, M. W. W. & Eidsness, M. K. (1998). *J. Biol. Inorg. Chem.* **3**, 484–493.
Campbell, J. W., Habash, J., Helliwell, J. R. & Moffat, K. (1986). *Daresbury Inf. Quart. Protein Crystallogr.* **18**, 23.
Chatake, T., Kurihara, K., Tanaka, I., Adams, M. W. W., Jenney, F. E., Tsyba, I., Bau, R. & Niimura, N. (2002). *Appl. Phys. A*, **74**, S1280–S1282.
Dauter, Z., Wilson, K. S., Sieker, L. C., Moulis, J. M. & Meyer, J. (1996). *Proc. Natl Acad. Sci. USA*, **93**, 8836–8840.
Evans, P. (1997). *Proceedings of the CCP4 Study Weekend. Recent Advances in Phasing*, edited by K. S. Wilson, G. Davies, A. W. Ashton & S. Bailey, pp. 97–102. Warrington: Daresbury Laboratory.
Fiala, G. & Stetter, K. O. (1986). *Arch. Microbiol.* **145**, 56–61.
Helliwell, J. R., Habash, J., Cruickshank, D. W. J., Harding, M. M., Greenhough, T. J., Campbell, J. W., Clifton, I. J., Elder, M., Machin, P. A., Papiz, M. Z. & Zurek, S. (1989). *J. Appl. Cryst.* **22**, 483–497.
Hernandez, G., Jenney, F. E. Jr, Adams, M. W. & LeMaster, D. M. (2000). *Proc. Natl Acad. Sci. USA*, **97**, 3166–3170.
Hiller, R., Zhou, Z. H., Adams, M. W. & Englander, S. W. (1997). *Proc. Natl Acad. Sci. USA*, **94**, 11329–11332.
Jenney, F. E. Jr & Adams, M. W. W. (2001). *Methods Enzymol.* **334**, 45–55.
Kurihara, K., Tanaka, I., Adams, M. W. W., Jenney, F. E. Jr, Moiseeva, N., Bau, R. & Niimura, N. (2001). *J. Phys. Soc. Jpn Suppl. Sect. A*, **70**, 400–403.
Langan, P., Greene, G. & Schoenborn, B. P. (2004). *J. Appl. Cryst.* In the press.
Langan, P. & Greene, G. (2004). Submitted.
Pflugrath, J. W. (1999). *Acta Cryst.* D**55**, 1718–1725.
Zartler, E.R., Jenney, F. E. Jr, Terrell, M., Eidsness, M. K., Adams, M. W. W. & Prestegard, J. H. (2001). *Biochemistry*, **40**, 7279–7290.